JOURNAL OF MATERIALS SCIENCE **38** (2003) 1321 – 1331

Chemically induced residual stresses in dental composites

P. LINGOIS
Division of Polymer Engineering, Luleå University of Technology, 97187 Luleå, Sweden

L. BERGLUND
Royal Institute of Technology, Department of Fiber and Polymer Technology, DKV53, SE-100 44 Stockholm, Sweden
E-mail: Lars.Berlund@mb.luth.se

A. GRECO, A. MAFFEZOLI
Department of Materials Science, University of Lecce, 73100 Lecce, Italy

In several European countries, dental composites are replacing mercury-containing amalgams as the most common restorative materials. One problem with dental composites is residual stresses which may lead to poor performance of the restoration. In the present study, a combined modeling and materials characterization approach is presented and predictions compare well with experimental data on residual stresses. The model takes stress relaxation into account through the complete relaxation time spectrum of the resin. The approach allows for detailed parametric studies where resin and composite composition as well as cure conditions may be tailored with respect to residual stress generation.

1. Introduction

The field of restorative dental materials has traditionally been dominated by mercury-containing metals. In European countries, among those Sweden, dental composites are increasingly replacing metals as the dental material of choice. Dental materials are typically based on acrylates containing glass fillers at a volume fraction of 0.5–0.6. The viscous dental composite is placed in the tooth cavity and the polymerization reaction is initiated using a dental lamp, typically blue light. Free radical polymerization starts and the increase in degree of conversion is associated with a substantial decrease in volume of the polymer. Gelation occurs at much lower degree of conversion as compared with, for instance, epoxies. During typical conditions, gelation is accompanied by almost instantaneous vitrification where the polymer enters the glassy state. As a consequence, considerable residual stresses may develop in the tooth and in the filling material. Detrimental effects include tooth cracking and marginal leakage so that bacteria may enter at the interface between the tooth structure and the synthetic filling.

In the present study, the objective is to develop a combined modeling and materials characterization approach for prediction of residual stresses. Ultimately such a model may be implemented in a finite element code so that detailed predictions of the stress state in a tooth structure become feasible. Presently, we are concerned with the material descriptions. A model material is used so that filler volume fraction can be varied. In a previous paper [1], micro-mechanics models for composite materials have been used to predict elastic properties and volume change on the basis of constituent properties and their volume fractions. These micromechanical models have been included in the modeling done in the present study. An interesting application of this approach is in the tailoring of constituent properties and composition in order to optimize material properties. Experimental work has indicated strong stress relaxation effects in dental composites and a viscoelastic material model is therefore included.

Previous modeling efforts for residual stresses in dental composites are limited in scope. Several are based on assumptions of elastic material behavior [2–7]. In a recent paper [8], FEM is applied to evaluate the stress state in a tooth structure containing a dental composite restoration. Although the material is described as viscoelastic, the description is simpler than ours, partly because the primary objective is to evaluate a given structure with respect to the final residual stress state at different locations. Our primary interest is instead in residual stress development with time. We develop a model where we can evaluate effects from cure kinetics, cure conditions, temperature, matrix viscoelasticity, resin and filler elastic constants, non-linear matrix shrinkage and filler volume fraction.

2. Experimental procedure

2.1. Materials

The resin was prepared from a 1:1 weight ratio mixture of Ebecryl® 610 from UCB Chemicals, Belgium, and Triethyleneglycol dimethacrylate (TEGDMA) from Aldrich Chemicals. The photoinitiator system

consisted of 1 wt% of camphorquinone (CQ) and 0.08 wt% of N,N-dimethyl-p-toluidine (DMPT), both were provided by Aldrich Chemicals. All chemical products were used as received.

The proportion of CQ was chosen carefully in order to minimize the gradient of degree of conversion for 1 mm thick samples. Indeed, since CQ absorbs light, the top and the bottom of the sample will not receive the same radiation energy, leading to differences in degree of conversion α. A low quantity of CQ would produce homogeneous α, but the reaction would be too slow. The concentration chosen provides a reasonably homogeneous degree of conversion in 1 mm thick samples with a fast reaction.

The filler was Spheriglass® from Potters and Ballotini, grade 5000 (solid glass spheres, mean diameter 3.5–7 microns, silanised for acrylate systems). The filler content was varied between 0–55 vol%.

2.2. Dynamic mechanical analysis

The resin was degassed at room temperature to remove entrapped air. It was then poured in a Teflon mould with the following dimensions: $1 \times 24 \times 50$ mm. Polyethyleneterephtalate (PET) films were placed on top and bottom of the mould. The sample was light cured with a Dulux S/E 9 W/71 lamp which has a high output spectrum in the blue range. One face of the samples was irradiated at a distance of 7 mm; the exposition time ranging from 15 s to 7 min in order to obtain different degrees of conversion. After irradiation, the samples were left one month in dark conditions at room temperature. The samples were then cut and polished to the final dimension, approximately $1 \times 3 \times 37$ mm.

The instrument used was a DMTA MK II from Polymer Laboratories. The samples were tested in tension. A step temperature program was used where isothermals are separated by 8°C. The complex modulus was measured during the isothermal for five frequencies, 0,3-1-3-10-30 Hz. The start temperature was different for each specimen and was between -100 and 0°C; the test was performed until the sample failed.

2.3. Differential scanning calorimetry

Cure kinetics was studied using a Perkin Elmer DSC 7 differential scanning calorimeter (DSC). The standard lids furnace was replaced by two quartz plates, in order to irradiate the reactive mixture in open sample pans. The lamp used for curing samples for DMTA and residual stress measurements was used operating in static air. The maximum heat of reaction $\Delta H = 150$ J/g was measured using a thermal initiator (Benzoyl Peroxide) during a DSC scan at 10°C/min. Measurements of the degree of conversion, α, as a function of time at 30-40-50-60-70°C were used in order to determine the kinetic parameters of the model. The isothermally cured samples of known final degree of reaction were subjected to a dynamic DSC scan in order to estimate their glass transition temperature (T_g) and residual reactivity. The T_g of highly crosslinked polymers is not easily observed using DSC and hence the onset of residual reactivity (T_{onset}) was assumed to correspond to the T_g. In fact, the residual reactivity in DSC heating scans was observed when the temperature reached the T_g of the resin. At this point, molecular mobility increased and reaction of residual double bonds commenced [9, 10]. The radical needed for the residual reactivity, originated during light exposure and can remain entrapped but active for more than one week [11]. Residual reactivity is not desired for DMTA experiments and hence the samples were stored in dark conditions for a month. After this period, a DSC scan performed on DMTA samples confirmed the lack of any residual reactivity.

T_{onset} is closely related to the glass transition temperature, T_g, so it is not surprising that we observed $T_{\text{onset}} = f(\alpha)$ to be linear. Indeed Maffezoli *et al.* [9] observed it for T_g for methacrylate dental resins, in agreement with other workers [12, 13].

Due to the temperature increase during curing, α of the DMTA samples had to be measured experimentally. The T_{onset} was determined of a sample prepared under the same conditions as a DMTA sample. When T_{onset} is above room temperature, it has been observed to correspond with the temperature, $T_{\tau_p^E}$, at which the relaxation spectrum, obtained with DMTA, has its maximum. For this reason, $T_{\tau_p^E}$ was assumed equal to T_{onset} even if no reaction can be observed after one month. The degree of conversion, α, of the DMTA samples was then determined from the T_{onset} versus α curve.

2.4. Matrix shrinkage measurements

Some pure resin was degassed and then three small drops were deposited on a flat metal surface, on which a thick layer of grease was applied to avoid any adhesion. The sample was light cured for 7 minutes with a Dulux S/E 9 W/71 lamp at a distance of 7 mm. A digital camera recorded the sample dimensions during curing. Then images taken at different time were analyzed to determine the change in diameter taken as the linear shrinkage. The degree of cure was determined using the cure kinetics model assuming isothermal conditions at the ambient temperature measured for each experiment.

2.5. Residual stress measurement

Compared with the bimaterial experiment previously used by Feilzer *et al.* [14], the experiment was improved in order to obtain the evolution of stress during curing (strain gauge methodology). The set-up is illustrated in Fig. 1.

The composite mixture was degassed at room temperature in order to remove any air bubbles. Then it was poured on an aluminum substrate surrounded by plasticine walls forming a temporary mold. Two strain gauges, CEA-13-240UZ-120 from the Measurements group, were bonded to the substrate and a thermocouple was taped centrally, between the strain gauges, at the aluminum substrate bottom, see Fig. 1. The aluminum substrate had the following dimensions: $1 \times 20 \times 70$ mm. The thickness of the composite mixture was approximately 0.7 mm. A PET film was placed on top and the sample was light cured for 7 minutes with a Dulux S/E 9 W/71 lamp at a distance of 7 mm.

The strain gauges were connected to a quarter Wheatstone bridge of an amplifier. The data were then converted to digital format and saved in a computer.

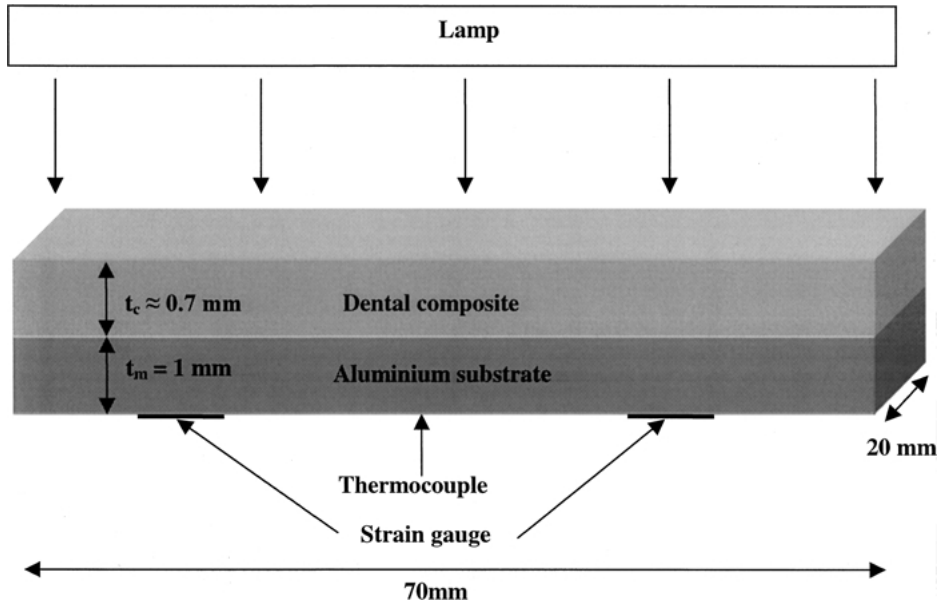

Figure 1 Experimental set-up for measurement of residual stress.

3. Data reduction

3.1. DMTA experiment

From the experiment we obtained the storage modulus at different temperatures for different frequencies. For modeling purposes we need Young's modulus as a function of time. Time-temperature superposition [15], commonly applied in viscoelasticity theory, was therefore used in order to determine the shift function at a reference temperature of 55°C, the chosen temperature of the isothermal model for pure resin. For the time-temperature superposition procedure, data should be corrected by

$$\frac{\rho}{\rho_0}\frac{T}{T_0} \tag{1}$$

where T is the temperature of the isothermal, T_0 is the reference temperature, ρ is the density at T, and ρ_0 is the density at T_0. The density ratio has been neglected because the variation of the density as a function of temperature is unknown but considered to be small [15].

From the time-temperature superposition procedure, we obtain the change in storage modulus as a function of time; what we need in our master model is the relaxation modulus as a function of time. The relaxation modulus was obtained using the following approximation [16]:

$$E(t) \approx E'(\omega)|_{\omega = 2/\pi t} \tag{2}$$

where E is the Young's modulus, E' is the storage modulus, and ω is the frequency. This expression was chosen for its simplicity and because it gives a good approximation [16].

3.2. Residual stress

From the bimaterial experiment, we obtain the strain in the substrate. Since the stress state in the material is two-dimensional, plate theory was used in order to obtain the residual stress in the material from the strain in the substrate. The substrate is considered infinitely rigid and the shear deformation between the free "top" surface of the dental composite and the constrained "bottom" surface is assumed negligible. Based on classical plate theory, the following equations were developed:

$$\varepsilon = \left[\frac{t_c + t_m}{2} - \frac{\left[\frac{t_m^2}{6} + \frac{t_c^2}{2} + \frac{t_c t_m}{2}\right] + \frac{E_c(1-\nu_m)}{E_m(1-\nu_c)}\frac{t_c^3}{6t_m}}{t_c + t_m}\right] k$$

$$\sigma = \frac{\frac{E_m t_m^3}{(1-\nu_m)} + \frac{E_c^2(1-\nu_m)}{E_m(1-\nu_c)^2}\frac{t_c^4}{t_m} + \frac{E_c}{1-\nu_c}t_c\left(4t_m^2 + 4t_c^2 + 6t_c t_m\right)}{6(t_c + t_m)t_c} k \tag{3}$$

where ε is the measured strain, k is the curvature, E is the Young's modulus, ν is the Poisson's ratio, t is the thickness, σ is the stress, and the subscripts m and c refer to the metal and composite respectively.

4. Modeling

Modeling of residual stresses under isothermal conditions requires a set of interacting submodels, see Fig. 2. The first submodel is the cure kinetics model. This model predicts the degree of conversion α as a function of time and temperature for the resin. In the present study, we use the same light intensity during curing, so this variable is excluded.

The temperature-time history during processing in combination with the cure kinetics model then provide us with the development in degree of conversion. In two additional submodels, the degree of conversion is related to the volume change and to the stiffness of the resin (see the two boxes in Fig. 2). Note that in the present study we only need to consider the case of strain in one direction.

A realistic model also needs to include viscoelastic effects. A viscoelastic model is therefore needed which can predict the reduction in Young's modulus of the resin with time under stress at a given temperature and degree of conversion. By comparison between the

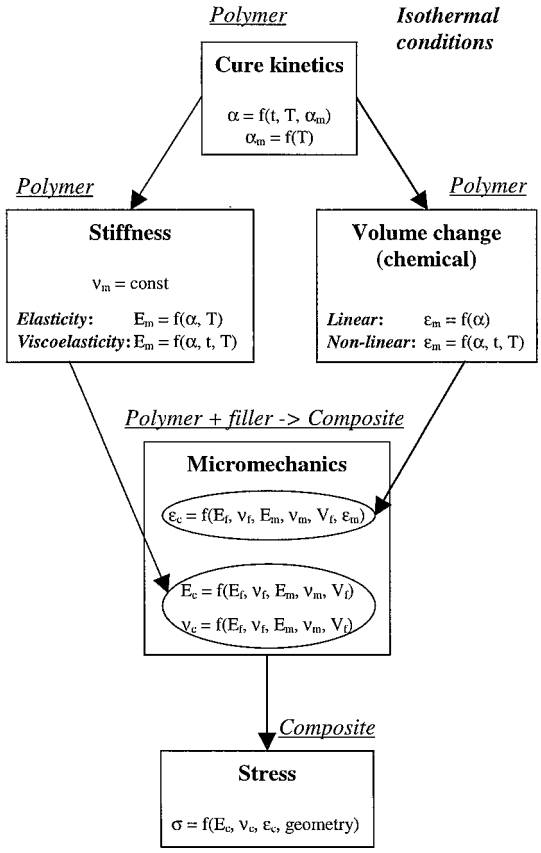

Figure 2 Overall modeling scheme illustrating the different submodels.

elastic and viscoelastic case, the viscoelastic contribution may be estimated. It will be shown later that a nonlinear shrinkage model including vitrification effects is also necessary.

We then combine the models for polymer behavior with micromechanics models (see the micromechanics frame in Fig. 2) in order to predict volume shrinkage and stiffness properties of the composite for any filler volume fraction.

Finally, having determined the chemically induced volume change and the stiffness of the composite, the residual stresses can be calculated using a stress model, see Fig. 2. This model gives us the residual stress in the dental composite for the bimaterial experiment chosen in the present study. Models are presented in the following whereas model parameters are presented in Table I.

TABLE I Parameters for modeling of the composite

E_f (GPa)	72
ν_f	0.22
ν_m	0.37
Log (E_u) (Pa)	$-0.870 * \alpha + 10.048$
Log (E_∞) (Pa)	$2.368 * \alpha + 6.478$
Log (a_T) = Log (τ_p^E) (s)	$-74{,}91 * (T - T_{\tau_p^E})/(366.07 + T - T_{\tau_p^E})$
$T_{\tau_p^E}$ (°K)	$148 + 340.4 \times \alpha$
$\Delta\varepsilon_m^\infty$ (%)	−5.9
K_0 (s^{-1})	0.1333
m	0.5271
n	1.4618
E_a (J/mol)	853.44
α_m	$-.06389 + .001896 * T$

4.1. Cure kinetics

The degree of conversion as function of time was obtained by solving a simple pseudo-autocatalytic equation [9]:

$$\begin{aligned} d\alpha/dt &= K_0 \exp(-E_a/RT)\alpha^m(\alpha_m - \alpha)^n \\ \alpha_m &= f(T) \end{aligned} \tag{4}$$

where K_0 is the pre-exponential factor of the rate constant, R is the gas constant, E_a is the activation energy, T is the absolute temperature, α_m is the maximum degree of reaction for the temperature T, m and n are fitting parameters independent of temperature, and f is an unknown function. Isothermal DSC experiments were carried out in order to determine the material constants, m and n, and the unknown function, f, in Equation 4. The procedure was previously applied to dental composites by Maffezoli *et al.* [9].

4.2. Stiffness: viscoelasticity

We then need a model for the change in viscoelastic behavior from the rubbery state, through the glass transition region and into the glassy state. Considering the present isothermal case, the following model was chosen for the viscoelastic Young's modulus of the matrix, E_m [17], as a function of time, temperature and degree of conversion. The particular choice is primarily based on the fact that our polymer has a broad relaxation time distribution.

$$\begin{aligned} E_m(\alpha, t, T) = E_\infty(\alpha) + (E_u(\alpha) - E_\infty(\alpha)) \\ \times \sum_{i=1}^{29} W_i \exp\left[\frac{-t}{\tau_p^E(\alpha, T)10^{i-15}}\right] \end{aligned} \tag{5}$$

where E_∞ is the relaxed modulus, E_u is the unrelaxed Young's modulus, W_i are weight factors, τ_p^E is the principal relaxation time (the time at which the relaxation spectrum has its maximum), t is the time, T is the temperature, and α is the degree of conversion. In theory, the weight factors depend on the degree of conversion. As demonstrated in the results section, W_i is independent of α in our case, so we obtain a single master curve. To find the weight factors, nonlinear curve fitting of the master curve was performed using the Levenberg-Marquardt method [18].

From time-temperature superposition theory, τ_p^E is related to the shift function, a_T, by the following relation:

$$\tau_p^E(\alpha, T) = \tau_p^E(\alpha, T_{\text{ref}})\, a_T(T, T_{\text{ref}}) \tag{6}$$

where T_{ref} is a reference temperature. If we chose $T_{\text{ref}} = T_{\tau_p^E}$, then $\tau_p^E(\alpha, T_{\text{ref}}) = 1$ second independent of α. The classical WLF equation was chosen to describe the shift function $a_T(T, T_{\text{ref}})$. As discussed previously $T_{\tau_p^E} = T_{\text{onset}}$ which experimentally was found to be linearly related to α.

The Poisson's ratio, ν_m, was assumed constant. Beckwith [19] measured the Poisson's ratio of neat epoxy during a low strain creep test and no appreciable

time-dependence of the Poisson's ratio was observed. Moreover, the model of Bogetti and Gillespie [20], used for residual stress predictions in fiber composites, contains a Poisson's ratio independent of the degree of conversion. They compared their model with the model of Levitsky and Shaffer [21–23] which assumes a constant bulk modulus (Poisson's ratio varies). They concluded that the model predictions converged very rapidly as the degree of conversion increased for a thermoset polyester. We therefore assumed Poisson's ratio to be independent of time and degree of conversion. The value for ν_m from ref. [1] was used.

4.3. Stiffness: elasticity

For elastic property modeling it was assumed that the dynamic modulus determined at 1 Hz is the elastic modulus, $E_m \cdot E_m$ was represented by an expression similar to Equation 5 except that the time is constant and equal to 1 second:

$$E_m(\alpha, T) = E_\infty(\alpha) + (E_u(\alpha) - E_\infty(\alpha)) \times \sum_{i=1}^{29} W_i \exp\left[\frac{-1}{\tau_p^E(\alpha, T)10^{i-15}}\right] \quad (7)$$

with the same notation as in Equation 5.

As for the viscoelastic case, ν_m is considered independent of the degree of conversion.

4.4. Volume change

In order to calculate stresses in our case, we only need the linear strain of the matrix, ε_m, rather than the volume change, ΔV. The relationship between these parameters is the following:

$$\Delta V = (1 - \varepsilon_m)^3 \quad (8)$$

where ε_m is considered positive for contraction.

The linear strain is a function of the degree of conversion. Since vitrification occurs during curing, strain is also a function of time and temperature. A non-linear model similar to the one for the Young's modulus was used to model shrinkage as a function of degree of conversion:

$$\Delta\varepsilon_m(\alpha, t, T) = \Delta\varepsilon_m^\infty + \left(-\Delta\varepsilon_m^\infty\right) \times \sum_{i=1}^{29} W_i \exp\left[\frac{-t}{\tau_p^\varepsilon(\alpha, T)10^{i-15}}\right] \quad (9)$$

where $\Delta\varepsilon_m$ is analogous to a shrinkage coefficient since it describes the slope of the linear shrinkage versus α, $\Delta\varepsilon_m^\infty$ is the shrinkage coefficient in the equilibrium state, W_i are weight factors, τ_p^ε is the principal relaxation time, t is the time, and α is the degree of conversion. The same weight factors as for the Young's modulus were chosen. This non-linear model is used in combination with the viscoelastic model for the Young's modulus.

In combination with the elastic Young's modulus the following linear model was used:

$$\Delta\varepsilon_m(\alpha) = \Delta\varepsilon_m^\infty \quad (10)$$

It is of interest to also consider a linear shrinkage model in the viscoelastic calculations. It then becomes possible to estimate the importance of the nature of the shrinkage model. In the context of viscoelasticity theory, linear shrinkage as a function of time follows from the following equation:

$$\varepsilon_m(t) = \int_0^t \Delta\varepsilon_m(\alpha, t - \theta, T)\frac{\mathrm{d}\alpha(\theta)}{\mathrm{d}\theta}\mathrm{d}\theta \quad (11)$$

where θ is an integrating variable.

4.5. Micromechanics modeling of the composite

The aim is predictions of stresses for different filler contents in the composite. For this reason, the properties of the pure resin were determined and then micromechanical models were used to determine composite properties from resin and filler properties.

The volume change for the composite due to matrix chemical shrinkage was determined using a micromechanical model developed by Levin for thermal expansion and reviewed in [24]. This model was used since the volume change problem is analogous to the thermal expansion problem, as discussed in [1]. In the present case, the volume change of the filler is zero since the temperature is constant. The volume change is therefore

$$\varepsilon_c = \frac{\varepsilon_m}{(1/K_m - 1/K_f)}\left[\frac{1}{K_c} - \frac{1}{K_f}\right] \quad (12)$$

where K is the bulk modulus, ν is the Poisson's ratio, ε_m is the linear chemical shrinkage, the subscripts, c, f, and m refer to the composite, filler, and matrix respectively, and V_f is the volume filler content. The bulk modulus of the composite is obtained from Equation 10. The bulk modulus of the matrix was considered constant and equal to its final value.

The elastic modulus of the present dental material is well described by the upper bound of Hashin's composite spheres model [25] as is apparent from [1]. The procedure is to first determine the bulk modulus and the shear modulus in order to obtain the Young's modulus of the composite. The expressions are:

$$K_c = K_m + \frac{V_f(K_f - K_m)}{1 + (1 - V_f)\left[(K_f - K_m)/\left(K_m + \frac{4}{3}G_m\right)\right]}$$

$$G_c = G_m\left[1 + \frac{V_f}{1/(\gamma - 1) + A(1 - V_f) - V_f\left(1 - V_f^{2/3}\right)^2/\left(BV_f^{7/3} + C\right)}\right] \quad (13)$$

with

$$\gamma = G_f/G_m$$

$$A = \frac{2(4 - 5\nu_m)}{15(1 - \nu_m)}$$

$$B = \frac{10(1-\nu_m)}{21} \times \frac{(7-10\nu_f)(7+5\nu_m)-\gamma(7-10\nu_m)(7+5\nu_f)}{4(7-10\nu_f)+\gamma(7+5\nu_f)}$$

$$C = \frac{10}{21}(7-10\nu_m)(1-\nu_m)$$

where the notation are the same as in the previous equation.

The relaxed and unrelaxed Young's modulus for the composite were calculated using the upper bound of Hashin's composite spheres model. The weight factors and the principal relaxation times were assumed to be independent of the filler volume fraction. This assumption is based on experimental observations discussed by Hashin [26].

The Poisson's ratio for the composite was obtained from the bulk modulus and the upper bound of the shear modulus computed by Hashin's composites sphere model.

4.6. Stress model

In the two-dimensional (2D) case, for an infinitely rigid substrate under isothermal conditions, the axial residual stress in the material is obtained from elasticity theory [27]. Assuming a ν_c independent of t and α, we obtain:

$$\sigma(t) = \int_{t_{\text{gel}}}^{t} \frac{E_c(t-\theta,\alpha)}{1-\nu_c}\frac{\mathrm{d}\varepsilon_c(\theta)}{\mathrm{d}\theta}\mathrm{d}\theta \qquad (14)$$

where E_c is the Young's modulus, ν_c is the Poisson's ratio, ε_c is the strain induced by the chemical shrinkage, α is the conversion, t is the time, t_{gel} is the time to gelation, and the subscript c refers to the composite. t_{gel} is assumed to occur as α reaches $\alpha_{\text{gel}} = 0.1$. This is when the polymer gels, changing from the liquid to the solid, rubbery state. No stresses will form in the liquid state. The choice of $\alpha_{\text{gel}} = 0.1$ is based on values for α_{gel} reported in other studies on similar materials [11, 28, 29]. Furthermore, the final residual stress prediction was found to be fairly insensitive to the choice of α_{gel}. This is because the time during which the polymer is in the rubbery state is quite long, and in our case shrinkage does not generate large stresses in the rubbery state.

Equation 14 is conveniently integrated in the elastic case, but not in the viscoelastic case where therefore the differential form is used. Because of the representation chosen for the matrix Young's modulus, see Equation 5, the expression for composite modulus E_c is of a similar form. For this reason, we need to solve a set of differential equations, as shown below. We incorporate the form of E_c analogous to Equations 5 in 14 and then the resulting equation is differentiated, leading to Equation 15. The first one (15a) is for each weight factor and the second one (15b) is for the relaxed modulus.

$$\frac{\mathrm{d}\sigma_i}{\mathrm{d}t} + \frac{\sigma_i}{\tau_p 10^{i-15}} = \frac{E_u - E_\infty}{1-\nu} W_i \frac{\mathrm{d}\varepsilon_s}{\mathrm{d}t} \qquad (15a)$$

$$\frac{\mathrm{d}\sigma_\infty}{\mathrm{d}t} = \frac{E_\infty}{1-\nu}\frac{\mathrm{d}\varepsilon_s}{\mathrm{d}t} \qquad (15b)$$

The equations represented in 15 are solved using finite difference. The residual stress is determined as the sum of these results.

5. Results and discussion

5.1. Development of the model

The first submodel is the one for cure kinetics, see Fig. 2. Here we followed the procedure in ref. [9] for determination of model parameters from isothermal DSC scans. A necessary part of that model is the relationship between the maximum degree of conversion, α_m, at a given temperature and the isothermal cure temperature, T. This relationship arises because the polymer matrix vitrifies as its T_g reaches the temperature at which it is cured [30]. Because of the vitrification, reaction rates become very slow. We expect $\alpha_m = f(T)$ to have a similar shape as $T_g = f(\alpha)$ although T_g will have slightly higher values. The experimental data are presented in Fig. 3. As expected, a linear variation was found between α_m and T, as was also observed by Maffezoli *et al.* [9] for dental composites.

In the submodel for viscoelastic description of the material, we need to experimentally determine the effect of α on E_u and E_∞. The logarithms of E_u and E_∞ were found to depend linearly on α, see Fig. 4. These dependencies were used, see Table I. In Fig. 4,

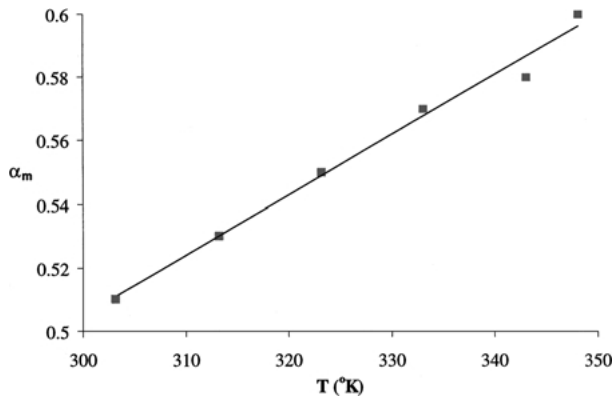

Figure 3 Data for maximum degree of conversion α_m as a function of isothermal cure temperature T (dark squares). The line represents the linear model fit.

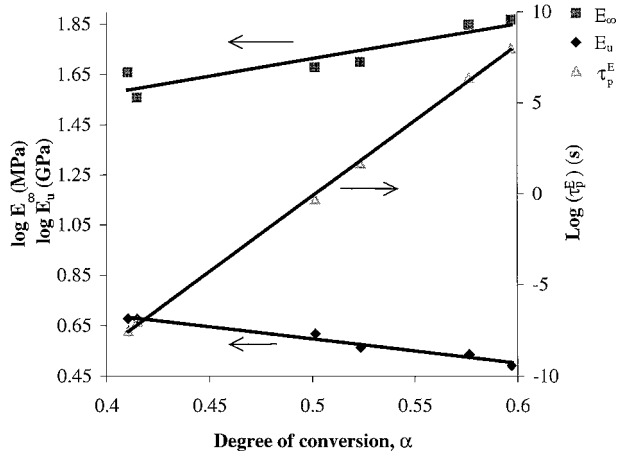

Figure 4 Logarithm of principal relaxation time τ_p^E, unrelaxed modulus E_u (GPa), and relaxed modulus E_∞ (MPa) as a function of degree of conversion α. The lines represent linear fits to data used in the models.

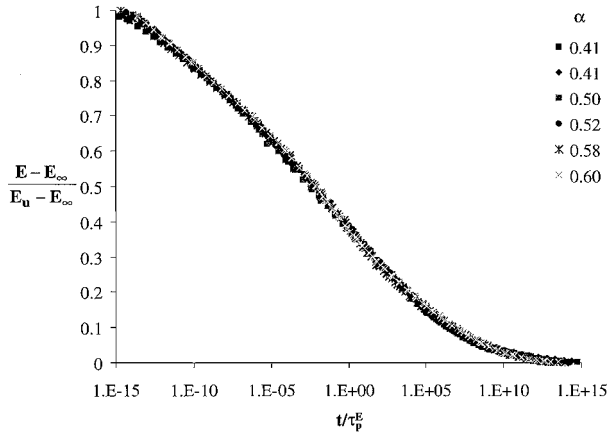

Figure 5 Reduced Young's modulus master curve as a function of reduced time. Data are for pure resin samples at different degree of conversion and have been shifted horizontally by τ_p^E.

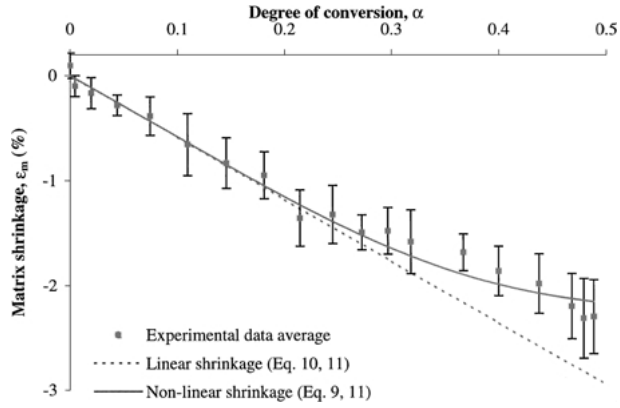

Figure 6 Measured shrinkage as a function of calculated degree of conversion. The shrinkage model and the initial linear shrinkage are also represented.

we also present predictions for τ_p^E based on Equation 6. There is good agreement between predictions and data which supports the validity of the expression for $\log a_T$ in Table I.

In Fig. 5, the reduced Young's modulus is presented for the resin. We may note that the relaxation time spectrum is very wide. The reason is the wide distribution of connectivity in this network polymer. In other words, the molecular network is inhomogeneous and different "linkages" have different lengths and relaxation times.

In the modeling section, we stated that the weight factors W_i in the viscoelastic model were found to be independent of α. Indeed, as the reduced Young's modulus, $(E - E_\infty)/(E_u - E_\infty)$, is plotted against the reduced time t/τ_p^E in Fig. 5, all data based on different α fall on a single master curve. This is an important aspect of the material behavior, since it allows us to use time-cure superposition theory. Time-cure superposition has been applied to network polymers previously [31–33] for long relaxation times. Adolf and Martin [34] were the first to develop a theory for the entire relaxation time spectrum of an epoxy system. Time-cure superposition is analogous to the classical time-temperature superposition theory in viscoelasticity. In time-cure superposition, the shifts in relaxation times result not from a change in molecular friction, but from a change in cross-link density. Normally the theory is valid in the critical regime near the gel point but not necessarily at reaction completion. However, their experimental data show that superposition is valid over at least half of the reaction. In our case, the data show that the theory is valid all the way from the glassy state to the rubbery state for samples that are quite far from the gel point. Consequently, time-cure superposition theory appears valid for acrylate systems over a wide range of α and not only near the gel point. In the study by Lange *et al.* on acrylate coatings, time-cure superposition was also applied although the verification was not complete [35]. The great advantage of time-cure superposition is that it allows the complete viscoelastic behavior of the system to be described from experimental "snapshots" at discrete times during the course of the reaction.

In Fig. 6, the shrinkage of the matrix as a function of the calculated degree of cure (cure kinetics model) is presented for the resin. It is clear that the shrinkage of the matrix is no longer linearly related to the degree of cure in the later stages, as the vitrification region is entered. This is in accordance with earlier observations [36, 37]. The non-linearity of the matrix shrinkage with degree of cure due to vitrification is an important phenomenon. Just to illustrate its importance, a linear model was also determined from the data, see Fig. 6 and Equation 11.

In our shrinkage model, the principal relaxation time (obtained from experiments), τ_p^ε, is 10^6 times the relaxation time for the Young's modulus, τ_p^E. This observation needs some further comments. It has been observed previously, that volume change and creep compliance have the same temperature dependence [38–40]. For this reason, we assume that volume change and relaxation modulus have the same dependence on degree of conversion. At the same time, we expect the volume change process to take more time. In support of this expectation, it has been observed that the maximum of the imaginary part of the dynamic bulk modulus occurs at a higher temperature than the maximum of the imaginary part of the dynamic shear modulus [41]. Volume relaxation therefore needs more time than shear relaxation, as is observed in our case.

The weight factors were considered identical to the weight factors of the Young's modulus. This assumption is supported by a previous study [42]. A stretched exponential function was used to fit dielectric and mechanical transitions of acrylate networks cured with UV light. The distribution parameter obtained from dielectric measurements was in very good agreement with the mechanical one and this for different degrees of conversion. Dielectric transitions are generally related to structural transitions, corresponding to changes in free volume or volume transitions. The volume and mechanical transitions are therefore considered to be similar in nature in this respect.

5.2. Comparison of residual stress predictions with experimental data

In Fig. 7, the effect of V_f on E_c and ε_c is shown as well as the residual stress, σ, calculated by the elastic and viscoelastic models at an isothermal temperature

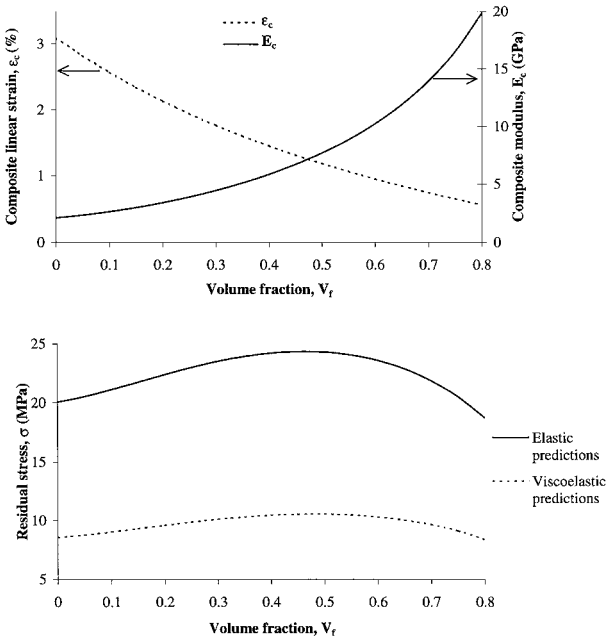

Figure 7 Modeling predictions. a) Composite shrinkage strain ε_c and composite modulus E_c as a function of volume fraction V_f. $T = 40°C$ and $\alpha = \alpha_{max.}$ b) Residual stress σ as a function of volume fraction V_f. Elastic and viscoelastic predictions. $T = 40°C$, $t = 7$ min.

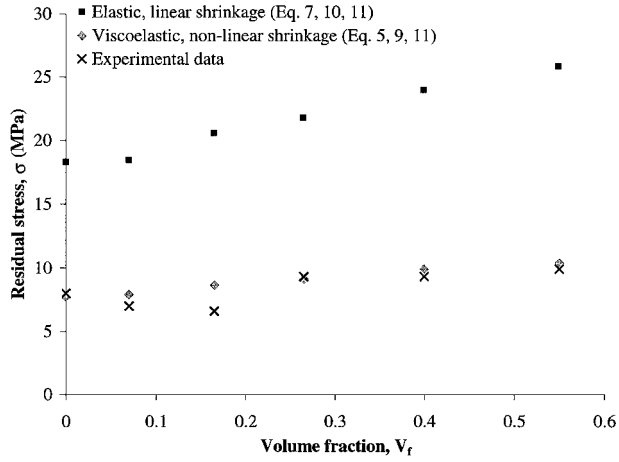

Figure 8 Residual stress σ as a function of volume fraction V_f. Predictions and data, $t = 7$ min. Temperatures of modeling correspond to experimental maximum temperatures.

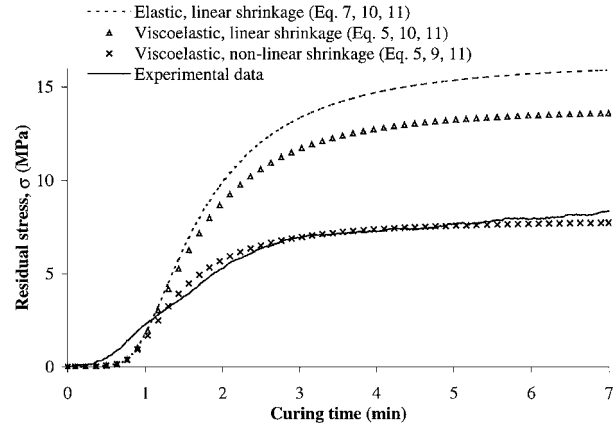

Figure 9 Residual stress σ as a function of curing time. Predictions and data are for the pure resin. $T = 55°C$.

of 40°C. The shapes of the curves differ slightly. For both models, predictions demonstrate a maximum in σ at a certain V_f. This V_f is the same for both models, around 0.45. The reason for the maximum is the different dependencies of composite modulus, E_c, and composite shrinkage, ε_c, on V_f. The effect of V_f is significant. With no filler, the residual stress in our experiment is 8 MPa whereas at $V_f = 0.45$ the stress is 11 MPa.

We may note that even at high V_f, the influence of viscoelastic relaxation effects is quite strong. An important conclusion is therefore that viscoelastic effects must be included in any analysis of residual stresses in dental composites. In the previously mentioned acrylate coating study by Lange *et al.* [35], the predicted viscoelastic effects were weaker than in our case. This is probably because the shrinkage model associated with their elastic predictions is non-linear and contains some viscoelastic effects. The importance of cross-link density was nicely demonstrated in ref. [35]. The moderately cross-linked acrylate showed much stronger relaxation effects than the densely cross-linked acrylate.

In Fig. 8, the elastic and the viscoelastic predictions for residual stress at the end of the 7 minutes of light curing are presented together with experimental data for composites of different V_f. Note that predictions in Fig. 8 are based on theoretical models and characterization of the polymer matrix only. Matrix and filler data are used to predict composite residual stress using theoretical models without fitting parameters.

Viscoelastic predictions are in good agreement with experimental data whereas elastic predictions are too high. Again, we conclude that viscoelastic relaxation effects during curing are very important. There is obviously great potential to exploit the relaxation effects in order to minimize the residual stress level in a dental composite. When the viscoelastic predictions were combined with the linear shrinkage model, Equation 11, predictions were between the two models in Fig. 8. The shortcomings with the linear model are discussed in connection with Fig. 9.

There was one practical difficulty with the residual stress experiments which we were unable to avoid. The exothermal heat of the curing reaction caused a temperature increase, whereas the analysis is isothermal. The maximum temperature measured at the bottom of the substrate of the bimaterial experiment was 46, 47.7, 44.2, 44.1, 40.6 and 34.8°C for V_f equals 0, 0.07, 0.165, 0.265, 0.4, 0.55 respectively. In order to compensate for this, the maximum temperature measured for each V_f was used for the isothermal predictions. In support of this simplification we observed that for the pure resin, the isothermal predictions and the experimental data have similar final degree of cure after 7 min of curing. A consequence of the different temperatures used in the predictions in Fig. 8 is that σ is higher at high V_f compared to Fig. 7 and the stress levels are slightly different. The decreased cure temperature at high V_f causes earlier vitrification and slightly higher stiffness of the glassy material. σ therefore becomes higher at high V_f.

In Fig. 9, residual stress as a function of time is presented for the neat resin. The experimental data are described by the solid line and the final residual stress for this specimen is 8 MPa. During the first 30 seconds, there is no stress development. Then follows a region in which the stress gradually increases and then levels off at around 3 minutes.

The elastic predictions based on linear shrinkage are much higher than experimental data. Predictions are also presented for the viscoelastic case with a linear shrinkage model. These predictions are lower than elastic predictions, but still much higher than experimental data. In contrast, the agreement is very good between data and viscoelasticity predictions using the non-linear shrinkage model.

The reason for the shortcomings of the linear shrinkage model is of interest. Even if this shrinkage model is adjusted so that the final shrinkage agrees with the experimentally measured shrinkage, stress predictions are wrong. The reason is that in residual stress modeling, the distribution of shrinkage during the curing process is very important. For instance, the extent of shrinkage is very large during the transition from the rubbery to the glassy state. However, in this region the relaxation effects are also dramatic. Because of this interaction between the shrinkage model and the viscoelastic relaxation model, correct predictions are very sensitive to the distribution of shrinkage as a function of degree of cure.

The first minute of the predicted residual stress development in Fig. 9 show very similar results for the three models. Then the models with linear shrinkage start to overestimate σ. The reason is that during this first minute, the resin is liquid and rubbery, so the Young's modulus and the shrinkage are the same for the three models. But as the material enters the glass transition region, shrinkage predictions become an important factor.

There is a deviation between data and viscoelastic predictions with non-linear shrinkage during the first minute. This is caused by the slightly non-isothermal conditions and the difference in thermal expansion between the strain gage and the substrate.

An interesting question is why the predicted stress in Fig. 9 increases so rapidly between 1 and 2 minutes. Also we may note that the difference between elastic and viscoelastic predictions do not really start until around 2 minutes for the linear shrinkage case. The reasons for these observations may be clarified from Fig. 10. Matrix modulus development with time is presented as well as the change in degree of conversion. The strong increase in E_m between 1 and 2 minutes explains the strong stress increase in this region. E_m increases because the polymer enters the glass transition region and E_m becomes dramatically higher than in the rubbery state.

The change in α with time is also of interest. At 1 minute, α is already about 0.35 but only low E_m exists (still rubbery state). Then as α goes from 0.35 to about 0.5, there is a strong increase in E_m since we enter the glass transition region. The matrix becomes glassy (vitrification) because T_g is approaching the cure

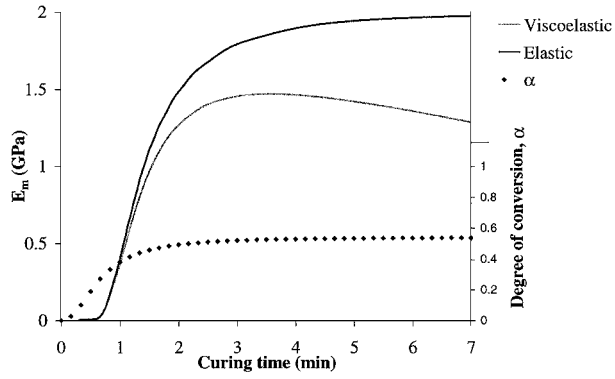

Figure 10 Predictions of matrix Young's modulus E_m (left axis) and degree of conversion α (right axis) as a function of curing time. E_m is based on elastic and viscoelastic models. $T = 55°C$.

temperature. Although we plot α, the vitrification phenomenon itself is the major factor generating residual stresses.

We may also note that the viscoelastic effects start to show around 1.5 minutes and then become increasingly larger with time (larger differences elastic-viscoelastic case). The significant decrease in modulus after 4 minutes is caused by the fact that we are still in the transition region at that temperature.

The strong but gradual increase in E_m between 1 and 2 minutes is related to the increase in α and the shape of the relaxation time spectrum in Fig. 5. We can then suggest two possibilities to reduce chemically formed residual stresses. Slow increase in α, by either slow cure kinetics of the resin or judicious choice of cure conditions, would allow more time for relaxation effects. The other possibility is by designing the network polymer in such a way that the relaxation time spectrum is more narrow. Such a polymer has higher relaxation rates in the transition region.

In practice, the intensity of the dental lamp is about 20 times higher than in our experiments. Then there is very little time for relaxation effects and the residual stresses actually developed should be closer to the predictions based on the elastic case.

6. Conclusions

A combined modeling and materials characterization approach was developed for prediction of chemical residual stresses σ in dental composites. The master model contains interacting submodels for cure kinetics, development of viscoelastic (or elastic) properties, volume change and stress development. The approach is micromechanical in nature, including effects from polymer characteristics as well as filler volume fraction V_f and particle properties on composite behavior. A key parameter is the degree of cure α, since development of viscoelastic properties and the volume change are controlled by α. From the model, development of α with curing time may be predicted as a function of resin cure kinetics, degree of cure, temperature, filler and matrix elastic properties, viscoelastic matrix properties, non-linear matrix shrinkage and V_f. The model takes stress relaxation into account through the

complete relaxation time spectrum of the resin. The model is also based on time-cure superposition theory and this was validated over a wide range of α for the acrylate system studied.

Predictions of σ as a function of V_f in a bimaterial set-up, demonstrated a maximum at $V_{f.} = 0.45$. The reason was the different dependencies of curing-induced volume change and increased modulus on V_f. Very high V_f, approaching 0.7, is therefore favorable from the point of view of residual stresses.

Viscoelastic model predictions of σ as a function of V_f were also found to agree very well with experimental data. This is very encouraging, since the model predictions are not based on any fitting procedure but rather on experimental data for the constituents combined with theoretical models. For improved predictive capability, extension of the model to non-isothermal conditions is required. The reason is the high reactivity of free radical cured dental composite resins, causing considerable heat generation even in small material volumes. Thermal strains due to differences in thermal expansion between enamel and the composite are also likely to be important.

Residual stress predictions based on elastic material behavior were twice as high as experimental data and viscoelastic predictions. This demonstrates that relaxation effects can be very strong. Viscoelastic stress relaxation effects can therefore be exploited in order to reduce residual stress levels.

An important submodel is the volume change (linear shrinkage in the present case) as a function of degree of cure. Our results demonstrate that the non-linear distribution of shrinkage during the curing process is critical to the predicted residual stresses. This is because of the interaction between the shrinkage model and the viscoelastic relaxation model. For instance, although the shrinkage is very large in the glass transition region, the resulting stresses are not so high due to correspondingly high relaxation rates.

In order to study the physics of the residual stress development process, the development of stress with time was predicted for a given case. In the early stages of curing, σ was low since the resin was in the rubbery state. In a narrow time interval, σ then increased rapidly. This was directly related to the increase in composite modulus E_c as the resin entered the glass transition region. In this stage α went from 0.35 to about 0.5. Comparison between elastic and viscoelastic predictions in this region again demonstrated the importance of stress relaxation effects and non-linear matrix shrinkage. This is the particular region where curing conditions could be controlled to maximize stress relaxation effects and reduce σ. The relaxation time spectrum of the resin is of major importance in this context and is controlled by the resin network structure. The model can therefore be applied to tailor not only cure conditions but also the relaxation time spectrum and cure kinetics of new resins in order to obtain favorable residual stress characteristics.

In practice, the intensity of the dental lamp is about 20 times higher than in our experiments. Then there is very little time for relaxation effects. The residual stresses actually developed would then be closer to the predictions based on the elastic case. However, modern lamps also allow for pulsed illumination. This provides new possibilities for controlled pauses so that the conditions for relaxation effects become favorable.

Acknowledgements

Financial support from the Swedish Engineering Research Council (TFR) is gratefully acknowledged. We are also grateful for helpful suggestions from Professors A. Apicella, University of Naples, Italy and K. J. Söderholm, University of Florida, Gainesville, USA. We wish to thank T. Olsson of the Wood Materials group at Luleå University of Technology for his help with the DMTA experiments.

References

1. P. LINGOIS and L. BERGLUND, *J. Mater. Sci.*, submitted.
2. J. HICKMAN, P. H. JACOBSEN, A. WILSON and J. MIDDLETON, *Clinical Materials* **7** (1991) 39.
3. P. F. HÜBSCH, J. MIDDLETON, J. S. REES and P. H. JACOBSEN, *J. Biomed. Eng.* **15** (1993) 401.
4. T. R. KATONA and M. M. WINKLER, *J. Dent. Res.* **73** (1994) 1470.
5. T. R. KATONA, M. M. WINKLER and J. J. HUANG, *Biomed. Mat. Res.* **31** (1996) 445.
6. M. M. WINKLER, T. R. KATONA and N. H. PAYDAR, *J. Dent. Res.* **75** (1996) 1477.
7. J. S. REES and P. H. JACOBSEN, *J. Dent.* **26** (1998) 361.
8. P. F. HÜBSCH, J. MIDDLETON and J. KNOX, *Biomaterials* **21** (2000) 1015.
9. A. MAFFEZOLI, R. TERZI and L. NICOLAIS, *J. Mater. Sci. Mater. Med.* **6** (1995) 155.
10. J. M. KENNY, A. MAFFEZZOLI and L. NICOLAIS, *Compos. Sci. Tech.* **38** (1990) 339.
11. J. G. KLOOSTERBOER and G. F. C. M. LIJTEN, *Polym. Commun.* **28** (1987) 2.
12. T. G. FOX and S. LOSHAEK, *J. Polym. Sci.* **15** (1955) 371.
13. D. ALPERSTEIN, M. NARKIS, A. SIEGMAN and B. BINDER, *Polym. Eng. Sci.* **35** (1995) 754.
14. A. J. FEILZER, A. J. DE GEE and C. L. DAVIDSON, *J. Dent. Res.* **69** (1990) 36.
15. J. D. FERRY, in "Viscoelastic Properties of Polymers," 3rd ed. (Wiley, New York, 1980) ch. 11.A.
16. R. M. CHRISTENSEN, in "Theory of Viscoelasticity: An Introduction," 2nd ed. (Academic Press, New York, 1982) ch. 4.
17. Y. K. KIM and S. R. WHITE, *Polym. Eng. Sci.* **36** (1996) 2852.
18. A. R. GALLANT, in "Nonlinear Statistical Models" (John Wiley & Sons, New York, 1987).
19. S. W. BECKWITH, *J. Spacecraft* **21** (1984) 546.
20. T. A. BOGETTI and J. W. JR. GILLESPIE, *J. Comp. Mater.* **26** (1992) 626.
21. M. LEVITSKY and B. W. SHAFFER, *J. Appl. Mech.* **41** (1974) 647.
22. B. W. SHAFFER and M. LEVITSKY, *ibid.* **41** (1974) 652.
23. M. LEVITSKY and B. W. SHAFFER, *ibid.* **42** (1975) 651.
24. B. W. ROSEN and Z. HASHIN, *Int. J. Eng. Sci.* **8** (1970) 157.
25. Z. HASHIN, *J. Appl. Mech.* **29** (1962) 143.
26. Z. HASHIN, *Int. J. Solids Structures* 1970; 6:539–552.
27. A. PLEPYS, M. S. VRATSANOS and R. J. FARRIS, *J. Composite Structures* **27** (1994) 51.
28. J. LANGE, *Polym. Eng. Sci.* **39** (1999) 1651.
29. D. ALPERSTEIN, S. NARKIS, A. SIEGMANN and B. BINDER, *ibid.* **35** (1995) 754.
30. J. K. GILLHAM, J. A. BENCI and A. NOSHAY, *J. Appl. Polym. Sci.* **18** (1974) 951.
31. D. J. PLAZEK, *J. Polym. Sci.*, Part A-2 **4** (1966) 745.
32. Y.-W. CHAN and J. J. AKLONIS, *J. Appl. Phys.* **54** (1983) 6690.

33. J. G. CURRO and P. PINCUS, *Macromolecules* **16** (1983) 559.
34. D. ADOLF and J. E. MARTIN, *ibid.* **23** (1990) 3700.
35. J. LANGE, A. HULT and J.-A. E. MÅNSON, *Polymer* **37** (1996) 5859.
36. M. KINKELAAR and L. J. LEE, in Proceedings of the 46th Annual Conference of Composites Institute, February 1991, edited by The Society of the Plastics Industry Inc., session 6-A, p. 1.
37. O. SINDT, S. L. SIMON, G. B. McKENNA and E. LIANG, in Proceedings of the 56th Annual Technical Conference, ANTEC, April 1998, edited by Soc. Plast. Eng. Brookfield CT, USA, p. 1658.
38. A. J. KOVACS, *J. Polym. Sci.* **30** (1958) 131.
39. C. A. BERO and D. J. PLAZEK, *J. Polym. Sci.; Part B: Polym. Phy.* **29** (1991) 39.
40. A. ESPINOZA and J. J. AKLONIS, *Polym. Eng. Sci.* **33** (1993) 486.
41. R. S. MARVIN and J. E. McKINNEY, in "Physical Acoustics" Vol. II B, edited by W. P. Mason (Academic Press, New York, 1975) p. 165.
42. A. R. KANNURPATTI and C. N. BOWMAN, *Macromolecules* **31** (1998) 3311.

Received 3 December 2001
and accepted 21 November 2002